

# Perlecan, the major proteoglycan of basement membranes, is altered in patients with Schwartz-Jampel syndrome (chondrodystrophic myotonia)

Sophie Nicole<sup>1</sup>, Claire-Sophie Davoine<sup>1</sup>, Haluk Topaloglu<sup>2</sup>, Laurence Cattolico<sup>3</sup>, Duarte Barral<sup>1</sup>, Peter Beighton<sup>4</sup>, Christiane Ben Hamida<sup>5</sup>, Hadi Hammouda<sup>6</sup>, Corinne Cruaud<sup>3</sup>, Peter S. White<sup>7</sup>, Delphine Samson<sup>3</sup>, J. Andoni Urtizberea<sup>8</sup>, Franck Lehmann-Horn<sup>9</sup>, Jean Weissenbach<sup>3</sup>, Faycal Hentati<sup>5</sup> & Bertrand Fontaine<sup>1,10</sup>

Schwartz-Jampel syndrome (SJS1) is a rare autosomal recessive disorder characterized by permanent myotonia (prolonged failure of muscle relaxation) and skeletal dysplasia, resulting in reduced stature, kyphoscoliosis, bowing of the diaphyses and irregular epiphyses<sup>1</sup>. Electromyographic investigations reveal repetitive muscle discharges, which may originate from both neurogenic and myogenic alterations<sup>2,3</sup>. We previously localized the SJS1 locus to chromosome 1p34–p36.1 and found no evidence of genetic heterogeneity<sup>4,5</sup>. Here we describe mutations, including missense and splicing mutations, of the gene encoding perlecan (*HSPG2*) in three SJS1 families. In so doing, we have identified the first human mutations in *HSPG2*, which underscore the importance of perlecan not only in maintaining cartilage integrity but also in regulating muscle excitability.

We constructed a physical map of the region containing the SJS1 locus, between markers *D1S2725* and *D1S2702*, which consists of a continuous set of YAC and PAC clones. We identified three new polymorphic repeats and a previously described *Bam*HI restriction polymorphism (Fig. 1a), which we subsequently used in haplotype analysis in eight consanguineous SJS1 families. We refined the localization of the gene to a region of approximately 100 kb, flanked by *D1S2725* and *HSPG2Bam*HI (Fig. 1b). This interval contains the gene encoding perlecan, a heparan sulphate proteoglycan<sup>6</sup> highly expressed in basement membranes and cartilage<sup>7,8</sup>. Consistent with this expression profile is the phenotype of homozygous mice with a null mutation in the perlecan gene: they develop severe chondrodysplasia and deterioration of basement membranes in regions of increased mechanical stress<sup>9,10</sup>.

And so we considered *HSPG2* to be a good candidate gene.

*HSPG2* encodes an mRNA with a predicted ORF of 13,173 nucleotides (ref. 11). We first sequenced the *HSPG2* exon-intron junctions to design intronic primers and detected 3 additional introns located in exons 7, 18 and 81 (ref. 12), giving a total of 97 exons for *HSPG2*. We then sequenced all coding exons in three of the eight consanguineous SJS1 families under study (SJS1-A, SJS1-B and SJS1-H; Fig. 1b). We identified three different homozygous mutations in *HSPG2* in patients from the three pedigrees. All mutations co-segregated with the disease and none was found in over 200 control chromosomes. Because of the low incidence of SJS1 and common ethnic origins of the 8 families under investigation (Tunisia from SJS1-A to SJS1-C and Turkey from SJS1-D to SJS1-H), we expected to find one or more of

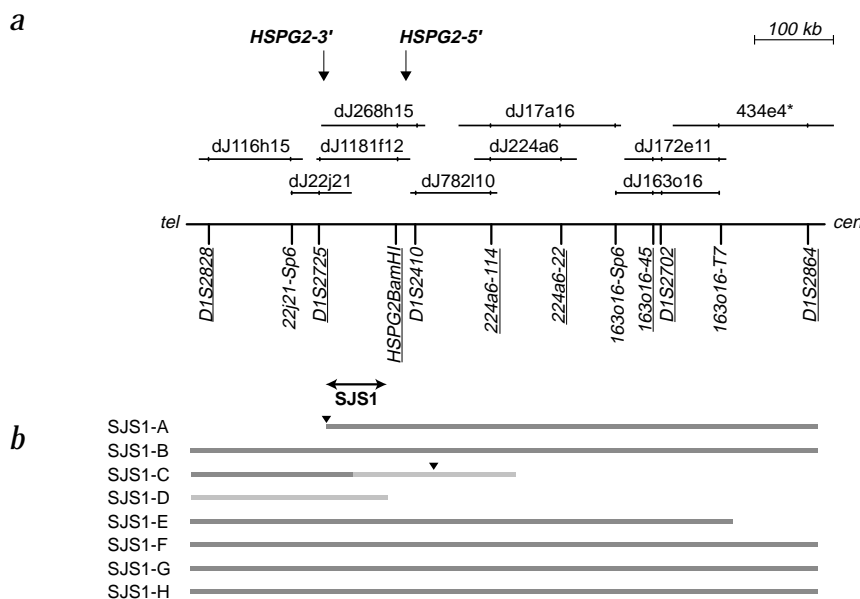


**Fig. 1** Physical map and genetic map of the SJS1 locus. **a**, The physical map is drawn with a minimal set of reagents. Positions of polymorphic markers (underlined), expressed sequences (bold) and STSs are indicated. Horizontal lines represent the YAC (\*) and PAC (dJ) clones allowing minimal covering of the critical region. The localization of *HSPG2* within the SJS1 critical interval was confirmed by amplification of exons 2 (*HSPG2*-5') and 97 (*HSPG2*-3'), and a *Bam*HI restriction polymorphism (*HSPG2Bam*HI), which resides in intron 6 of *HSPG2* (ref. 25). **b**, Schematic representation of regions segregating with the disease in 8 consanguineous SJS1 families. A homozygous region (dark grey box) was found in all affected patients, according to their consanguineous status. A light grey box indicates a uninformative homozygosity, as both parents were also homozygous. The recombination event (arrowhead) proximal to *D1S2725* in family SJS1-A and the heterozygosity of the SJS1-D proband for *HSPG2Bam*HI refined the critical region (SJS1) to approximately 100 kb.

<sup>1</sup>INSERM CjF9711, Faculté de Médecine Pitié-Salpêtrière, Paris, France. <sup>2</sup>Department of Paediatric Neurology, Hacettepe University, Faculty of Medicine, Ankara, Turkey. <sup>3</sup>Genoscope, Evry, France. <sup>4</sup>Department of Human Genetics, University of Cape Town, South Africa. <sup>5</sup>Institut National de Neurologie, Tunis, Tunisia. <sup>6</sup>Généthon, Evry, France. <sup>7</sup>Division of Oncology, Children's Hospital, Philadelphia, Pennsylvania, USA. <sup>8</sup>Institut de Myologie, Groupe Hospitalier Pitié-Salpêtrière, Paris, France. <sup>9</sup>Department of Physiology, University of Ulm, Ulm, Germany. <sup>10</sup>Fédération de Neurologie, Groupe Hospitalier Pitié-Salpêtrière, Paris, France. Correspondence should be addressed to B.F. (e-mail: [bertrand.fontaine@psl.ap-hop-paris.fr](mailto:bertrand.fontaine@psl.ap-hop-paris.fr))

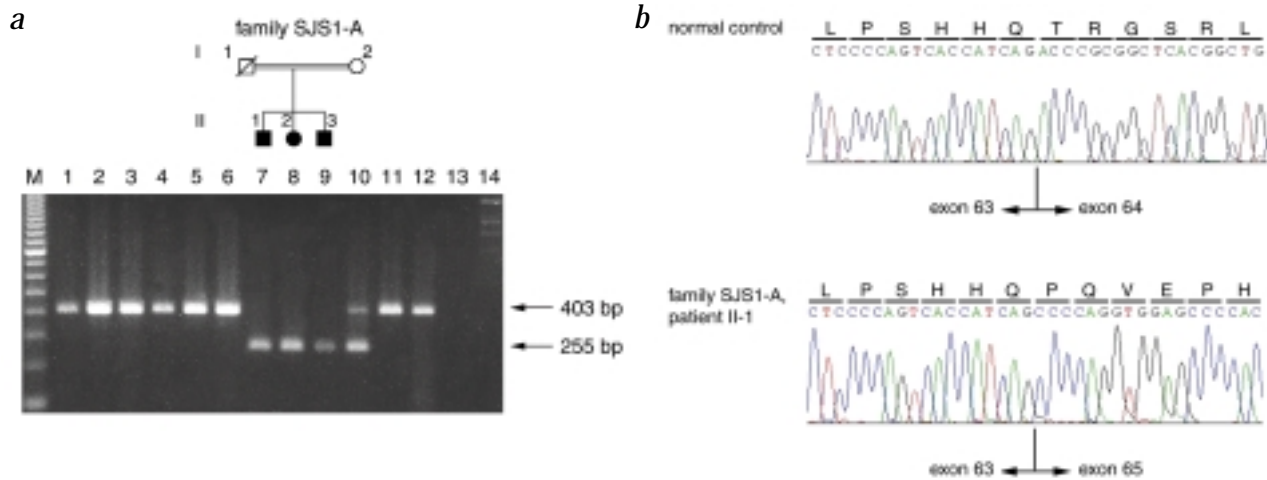


**Fig. 2** RT-PCR analysis of *HSPG2* exon-64 splicing event. **a**, Ethidium-stained agarose electrophoresis of RT-PCR products. An expected product of 403 bp was observed from all human control tissue samples whereas an abnormal product of 255 bp was observed in family SJS1-A. M, 100-bp ladder; lane 1, adult brain; lane 2, adult spinal cord; lane 3, adult skeletal muscle; lane 4, fetal skeletal muscle; lane 5, adult chondrocytes; lane 6, fetal chondrocytes; lanes 7–10, lymphoblastoid cell lines from family SJS1-A; lanes 11 and 12, lymphoblastoid cell line from normal controls; lane 13, water; lane 14, human genomic DNA. **b**, Sequence analysis of the 403-bp (normal control) and 255-bp (patient II-1) RT-PCR products demonstrating the loss of exon 64 sequence in mRNA from SJS1-A patients. This introduces a frameshift and a subsequent premature termination codon at 24 aa downstream from exon 64 skipping.

the mutations to be common. We tested the five remaining families (SJS1-C to SJS1-G) for the three identified mutations. None tested positive for the mutations, and so no major founder effect responsible for SJS1 in the eight families was observed.

We identified a homozygous A→G transition at position +4 of the intron 64 splice-donor site (IVS64+4a→g) in affected patients from kindred SJS1-A. Calculation of the consensus value (CV) at position –2 to +6, which reflects the similarity of one splice site to the consensus sequence<sup>13</sup>, revealed a lower CV for the mutated splice-donor site than for the wild-type equivalent (0.731 compared with 0.839). To determine the consequences of this splice-donor mutation, we carried out RT-PCR analysis, using primers that span exon 64 and lymphoblastoid cell lines from family SJS1-A and unrelated normal controls (Fig. 2a). Those derived from controls generated a fragment of expected size (403 bp), whereas a shorter product of approximately 255 bp was obtained from the cell lines derived from family SJS1-A. The mother's sample yielded both normal and shorter products, indicating a heterozygous status of the mutation. To confirm that the 255-bp product was not a normal splicing variant<sup>14</sup>, we sought its presence in various tissues that represent potential targets in SJS1 and were obtained from normal human controls. We found expression of *HSPG2* in all of them and the 255-bp cDNA product in none of them. Sequencing the 255-bp product revealed it to lack exon 64 (Fig. 2b). Loss of exon 64 in mRNA introduces a frameshift and a subsequent premature codon stop, predicted to result in a truncated protein lacking 1,595 amino acids. In family SJS1-B, we found a 4740G→A silent nucleotide change affecting the last nucleotide of exon 37. The corresponding

splice-donor site demonstrated a lower CV (0.702) than that of the wild-type site (0.826). This mutation presumably acts in a similar manner to IVS64+4a→g, although further verification was not possible because of the unavailability of lymphoblastoid cell lines

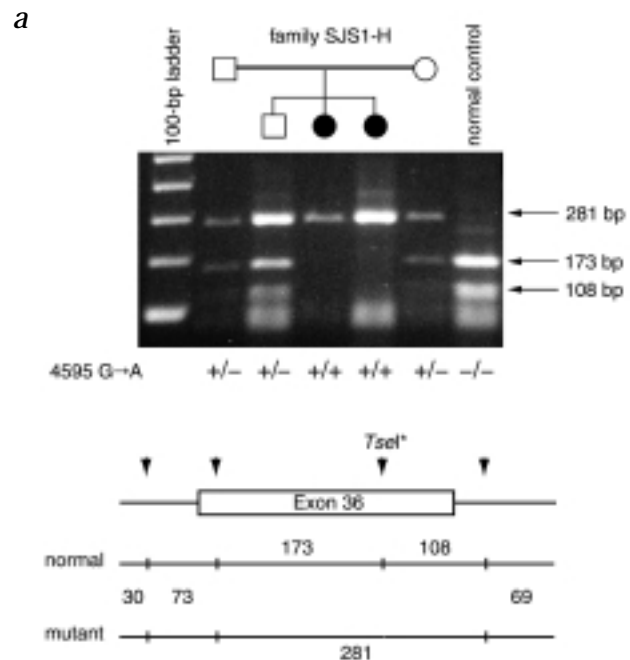
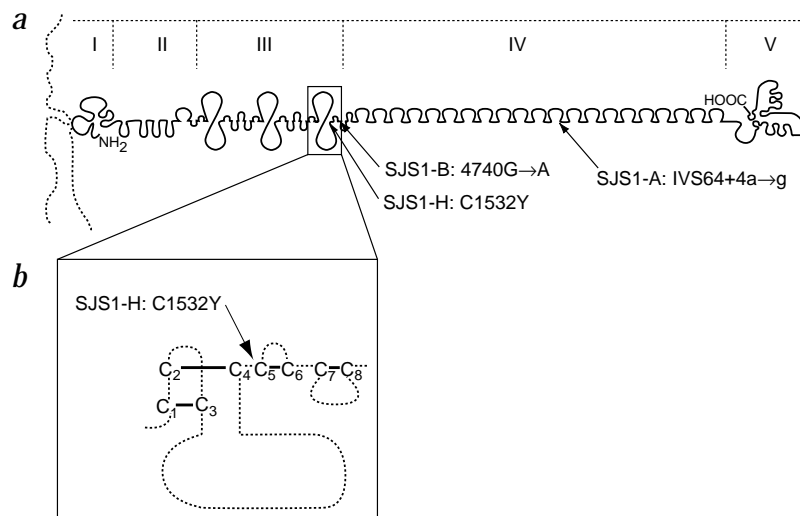


**Fig. 3** Mutation detection in family SJS1-H. **a**, The segregation of the 4595G→A transition was assayed by digestion with *Tsel*. The 453-bp PCR product encompassing exon 36 has three invariant *Tsel* recognition sites (▼). A fourth recognition site (*Tsel*\*) disappeared when the transition was present, leading to a 281-bp digestion fragment compared with the 173-bp and 108-bp bands observed for the wild-type allele. **b**, Alignment of the amino acid sequence of perlecan and laminin  $\alpha$ -1 from various species showing conservation of Cys1532. Conserved amino acids are shaded. The conservation of Cys1532 is presented in bold. The DNA sequences of the normal and mutant proteins are shown above and below the amino-acid sequences, respectively. *C. elegans* UNC-52, nematode orthologue of perlecan.

**Fig. 4** Predicted topology of perlecan and mutations in SJS1. **a**, The core protein of perlecan consists of five domains (I-V; adapted from ref. 26). Domain III is predicted to contain 15 cysteine-rich epidermal-growth-factor (EGF)-like regions, three of which contain an inserted cysteine-free sequence (globular motif). Two SJS1 mutations are located in exons encoding the C terminus of domain III. Domain IV contains 21 immunoglobulin (Ig)-like repeats resembling those of neural cell adhesion molecule (N-CAM). The IVS64+4a→g mutation is predicted to result in a truncated protein lacking Ig-like repeats 13-21 and domain V, which shares homologies with laminin  $\alpha$ -1. **b**, Predicted structure of the third globular motif of domain III (adapted from ref. 27), which is composed of a cysteine-free domain inserted within an EGF-like motif. An EGF-like motif contains 8 cysteine residues (C<sub>1</sub>-C<sub>8</sub>) forming 4 disulphide bonds (-). The missense C1532Y mutation affects the C<sub>5</sub> residue of the globular motif, likely abolishing the C<sub>5</sub>-C<sub>6</sub> bond. Exon 37, which is potentially affected in family SJS1-B, encodes a 38-aa fragment containing the C<sub>7</sub> and C<sub>8</sub> residues of the third globular motif and C<sub>1-4</sub> residues of the next EGF-like motif.



from family SJS1-B. In the last family studied (SJS1-H), we discovered a G→A nucleotide change at nt 4,595 that cosegregates with affected status (Fig. 3a). It predicts a substitution of tyrosine for cysteine (C1532Y); the cysteine residue is conserved across species in perlecan and laminin  $\alpha$ -1 (Fig. 3b), another extracellular matrix protein that has amino-acid homologies with perlecan<sup>11</sup>.

Perlecan binds to various basement membrane proteins, such as collagen IV and laminin-1, and to cell surface receptors, such as  $\beta$ 1-integrin and  $\alpha$ -dystroglycan<sup>15</sup>. Its core protein (of 4,391 aa) is composed of several modules arranged in five distinct domains (Fig. 4a). Two of the three mutations (C1532Y and 4740G→A) reside in domain III and probably lead to the loss of disulphide bonds, which may disrupt the conformation of this domain (Fig. 4b). The third SJS1 mutation (IVS64+4a→g) leads to a product lacking part of domain IV and the whole of domain V. The three mutations probably result in loss of function and therefore diminish integrity of cell basement membranes and cartilage matrix. Poor chondrocyte columnar organization and mild skeletal muscle dystrophic changes in patients with SJS1 support this assumption<sup>16,17</sup>. Nevertheless, the SJS1 phenotype is milder than that of the mutant mice, in which craniofacial abnormalities and a lethal deterioration of contracting myocardium are also observed. This discrepancy may be due to the different locations of loss-of-function mutations, which lead to a complete abolition of perlecan expression in mice and a putative preservation of the amino-terminal domains in patients with SJS1. Such a relationship has been observed for the gene encoding the *Caenorhabditis elegans* homologue of perlecan: loss-of-function mutations affecting domains II or III result in mortality of larvae, whereas those residing in domain IV lead to adult paralysis<sup>18</sup>.

More surprising is the association between myotonia and *HSPG2* mutations. Perlecan is present in endomysium, the connective tissue sheath surrounding individual skeletal muscle fibres<sup>19</sup>, whereas it is currently established that most myotonic disorders result from mutations in genes encoding voltage-gated ion channels<sup>20</sup>. The association of mutations in the perlecan gene with myotonia thus provides evidence for alternative mechanisms that lead to muscle hyperexcitability. One possible explanation could involve the modulation of ion-channel expression or function through their interaction with perlecan, as reported for tenascin-R, another extracellular matrix protein<sup>21,22</sup>. Another possibility has come to light following a study indicating that perlecan may be one component of the basal lamina required for synaptic clustering of acetylcholinesterase<sup>23</sup>. An abnormal accumulation of this enzyme, which is the primary terminator of

nerve impulse transmission at the neuromuscular junction, may result in lower acetylcholine degradation leading ultimately to muscle re-excitation and myotonia<sup>24</sup>.

## Methods

**Patient selection.** Families are described in ref. 5. We carried out our study after ethical review and in accordance with the Helsinki Convention and the relevant bioethics legislation of the participating countries.

**Construction of YAC and PAC contig.** Based on radiation hybrid data (<http://www.ncbi.nlm.nih.gov/genemap>), we used 54 sequence tagged sites (STSs) positioned within the SJS1 region to select YAC and PAC clones by scanning the Whitehead Institute ([http://www-genome.wi.mit.edu/cgi-bin/contig/phys\\_map](http://www-genome.wi.mit.edu/cgi-bin/contig/phys_map)) and the Sanger Centre (<http://www.sanger.ac.uk/HGP/search>) web sites. We closed some gaps in developing STSs from PAC-end-clone sequences, which we determined by direct sequencing of PAC clones according to the manufacturer's recommendations (Perkin-Elmer), and in screening PCR-DNA pools of the CEPH (YAC) and the RPCI-1 (PAC) human libraries to identify new genomic clones.

**Identification of repeat polymorphisms and genotyping.** We used the RepeatMasker program (<http://ftp.genome.washington.edu/RM/RepeatMasker.html>) to identify nucleotide repeats in sequence data from PACs dJ224a6 and dJ163o16 produced by the chromosome 1 sequencing group at the Sanger Centre. We generated primers from the sequences flanking the newly identified repeats to test their polymorphism. Markers were amplified using genomic DNA and fluorescent labelled primers. PCR products were separated on an ABI 377 DNA sequencer and the results analysed using Genotyper 2.0 software (Perkin Elmer). We studied the *Bam*HI polymorphic restriction site within *HSPG2* (*HSPG2BamHI*) as described<sup>25</sup>.

**Sequencing.** We carried out all sequences on an ABI 377 DNA sequencer (PE-Applied Biosystems) using BigDye Terminator chemistry (Perkin-Elmer).

**Mutation screening.** We first used 120 primers located in *HSPG2* exons according to the published *HSPG2* genomic organization, so as to determine intronic sequences flanking exons by direct sequencing PAC clone dJ268h15. We subsequently designed 92 pairs of intronic primers to amplify all exons (except exon 1; its high GC content prevented PCR amplification) and used them to amplify genomic DNA from both affected and unaffected family members. We carried out automated sequencing analysis using both forward and reverse PCR primers. Primer sequences are available on request. We determined the frequency of the observed nucleotide changes by sequence or enzymatic restriction analysis (NE Biolabs) of unrelated control chromosomes (European, North African and Turkish populations).

**RT-PCR analyses.** We extracted total RNA from human fetal skeletal muscle and lymphoblastoid cell lines using RNA-PLUS (Quantum Biotechnologies)

extraction solution. Total (brain and skeletal muscle) and poly(A)<sup>+</sup> (spinal cord) RNAs were purchased (Clontech). cDNA synthesis was carried out with random hexamers and *Thermoscript* reverse transcriptase (Life Technologies) on total RNA (4 µg) or poly(A)<sup>+</sup> RNA (100 ng), digested with RNase free DNase I (10 U; Roche Diagnostics). We amplified one fragment encompassing exon 64 with primers RT-HSPGEX62u (exon 62, 5'-CTCCATCGTCATCTCCGTCT-3', position 8,121-8,140) and RT-HSPGEX65l (exon 65, 5'-GTCTGCCCTTCTGCCACTC-3', position 8,528-8,510) or primers RT-HSPGEX63u (exon 63, 5'-GCCTCCCGAGTCCACATC-3', position 8,297-8,314) and RT-HSPGEX66l (exon 66, 5'-CCTGAGCTTCCGGTCACTT-3', position 8,699-8,681) in a standard 30-µl PCR reaction containing cDNA (1/10th of the cDNA synthesis). RT-PCR products were separated on a 1.5% agarose gel. We extracted the two RT-PCR products obtained from individual I-2 of family SJS1-A using the NUCLEOTRAP extraction kit (Macherey-Nagel) before sequencing.

**Sequence comparisons.** We carried out local alignment of amino-acid sequences using the LALIGNp program of the FASTA package (<http://www.infobiogen.fr/services/menuserv.html>) with default parameters.

**Accession numbers.** All *HSPG2* nucleotide positions refer to the coding sequence (GenBank M85289) with nucleotide +1 corresponding to the 'A' of

the first methionine codon. PAC dJ224a6, AL031281; PAC dJ163o16, AL031279; 224a6-114, AJ296644; 224a6-22, AJ296643; 163o16-45, AJ296645; human perlecan, translation of M85289; mouse perlecan, Q05793; *C. elegans* UNC-52, Q06561 and AAD25092; human laminin  $\alpha$ -1 chain precursor, P25391; mouse laminin  $\alpha$ -1 chain precursor, P19137; *HSPG2* exons and flanking intronic regions, AL445795-AL445846, AL445863.

#### Acknowledgements

We thank the patients, their families and the physicians for participation; A. Munnich for human chondrocyte RNA; the UK HGMP for PAC PCR pools of the RPC1-1 library and PAC clones; the Banque de Tissus pour la Recherche de l'Association Française contre les Myopathies (AFM-BTR) for skeletal muscle samples; the cell and DNA banks of the Institut National de la Santé et de la Recherche Médicale (INSERM) U289 and of the Groupe Hospitalier Cochin-Port Royal for lymphoblastoid cell lines and DNA samples; and N. Tabti for comments on the manuscript. S.N. was supported by grants from the Académie Nationale de Médecine and, subsequently, AFM. This work received financial support from AFM and INSERM (APEX).

Received 6 June; accepted 24 September 2000.

- Viljoen, D. & Beighton, P. Schwartz-Jampel syndrome (chondrodystrophic myotonia). *J. Med. Genet.* **29**, 58-62 (1992).
- Christova, L.G., Alexandrov, A.S. & Ishpekova, B.A. Single motor unit activity pattern in patients with Schwartz-Jampel syndrome. *J. Neurol. Neurosurg. Psychiatry* **66**, 252-253 (1999).
- Cadihac, J., Baldet, P., Greze, J. & Duda, H. E.M.G. studies of two family cases of the Schwartz and Jampel syndrome (osteo-chondro-muscular dystrophy with myotonia). *Electromyogr. Clin. Neurophysiol.* **15**, 5-12 (1975).
- Nicole, S. *et al.* Localization of the Schwartz-Jampel syndrome (SJS) locus to chromosome 1p34-p36.1 by homozygosity mapping. *Hum. Mol. Genet.* **4**, 1633-1636 (1995).
- Fontaine, B. *et al.* Recessive Schwartz-Jampel syndrome (SJS): confirmation of linkage to chromosome 1p, evidence of genetic homogeneity and reduction of the SJS locus to a 3-cM interval. *Hum. Genet.* **98**, 380-385 (1996).
- Iozzo, R.V. Matrix proteoglycans: from molecular design to cellular function. *Annu. Rev. Biochem.* **67**, 609-652 (1998).
- Hassell, J.R. *et al.* Isolation of a heparan sulfate-containing proteoglycan from basement membrane. *Proc. Natl Acad. Sci. USA* **77**, 4494-4498 (1980).
- SundarRaj, N., Fite, D., Ledbetter, S., Chakravarti, S. & Hassell, J.R. Perlecan is a component of cartilage matrix and promotes chondrocyte attachment. *J. Cell. Sci.* **108**, 2663-2672 (1995).
- Arikawa-Hirasawa, E., Watanabe, H., Takami, H., Hassell, J.R. & Yamada, Y. Perlecan is essential for cartilage and cephalic development. *Nature Genet.* **23**, 354-358 (1999).
- Costell, M. *et al.* Perlecan maintains the integrity of cartilage and some basement membranes. *J. Cell. Biol.* **147**, 1109-1122 (1999).
- Murdoch, A.D., Dodge, G.R., Cohen, I., Tuan, R.S. & Iozzo, R.V. Primary structure of the human heparan sulfate proteoglycan from basement membrane (*HSPG2/perlecan*). A chimeric molecule with multiple domains homologous to the low density lipoprotein receptor, laminin, neural cell adhesion molecules, and epidermal growth factor. *J. Biol. Chem.* **267**, 8544-8557 (1992).
- Cohen, I.R., Grassel, S., Murdoch, A.D. & Iozzo, R.V. Structural characterization of the complete human perlecan gene and its promoter. *Proc. Natl Acad. Sci. USA* **90**, 10404-10408 (1993).
- Shapiro, M.B. & Senapathy, P. RNA splice junctions of different classes of eukaryotes: sequence statistics and functional implications in gene expression. *Nucleic Acids Res.* **15**, 7155-7174 (1987).
- Noonan, D.M. & Hassell, J.R. Perlecan, the large low-density proteoglycan of basement membranes: structure and variant forms. *Kidney Int.* **43**, 53-60 (1993).
- Hopf, M., Gohring, W., Kohfeldt, E., Yamada, Y. & Timpl, R. Recombinant domain IV of perlecan binds to nidogens, laminin-nidogen complex, fibronectin, Fibulin-2 and heparin. *Eur. J. Biochem.* **259**, 917-925 (1999).
- Aberfeld, D.C., Hinterbuchner, L.P. & Schneider, M. Myotonia, dwarfism, diffuse bone disease and unusual ocular and facial abnormalities (a new syndrome). *Brain* **88**, 313-322 (1965).
- Ben Hamida, M., Miladi, N. & Ben Hamida, C. Schwartz-Jampel syndrome. Clinical and histopathological study of 4 cases. *Rev. Neurol. (Paris)* **147**, 279-284 (1991).
- Rogalski, T.M., Gilchrist, E.J., Mullen, G.P. & Moerman, D.G. Mutations in the *unc-52* gene responsible for body wall muscle defects in adult *Caenorhabditis elegans* are located in alternatively spliced exons. *Genetics* **139**, 159-169 (1995).
- Couchman, J.R. & Ljubimov, A.V. Mammalian tissue distribution of a large heparan sulfate proteoglycan detected by monoclonal antibodies. *Matrix* **9**, 311-321 (1989).
- Fontaine, B., Plassart-Schiess, E. & Nicole, S. Diseases caused by voltage-gated ion channels. *Mol. Aspects Med.* **18**, 415-463 (1997).
- Srinivasan, J., Schachner, M. & Catterall, W.A. Interaction of voltage-gated sodium channels with the extracellular matrix molecules tenascin-C and tenascin-R. *Proc. Natl Acad. Sci. USA* **95**, 15753-15757 (1998).
- Xiao, Z.C. *et al.* Tenascin-R is a functional modulator of sodium channel  $\beta$  subunits. *J. Biol. Chem.* **274**, 26511-26517 (1999).
- Peng, H.B., Xie, H., Rossi, S.G. & Rotundo, R.L. Acetylcholinesterase clustering at the neuromuscular junction involves perlecan and dystroglycan. *J. Cell. Biol.* **145**, 911-921 (1999).
- van Dijk, J.G., Lammers, G.J., Wintzen, A.R. & Molenaar, P.C. Repetitive CMAPs: mechanisms of neural and synaptic genesis. *Muscle Nerve* **19**, 1127-1133 (1996).
- Hansen, P.M. *et al.* Genetic variation of the heparan sulfate proteoglycan gene (*perlecan* gene). Association with urinary albumin excretion in IDDM patients. *Diabetes* **46**, 1658-1659 (1997).
- Kallunki, P. & Tryggvason, K. Human basement membrane heparan sulfate proteoglycan core protein: a 467-kD protein containing multiple domains resembling elements of the low density lipoprotein receptor, laminin, neural cell adhesion molecules, and epidermal growth factor. *J. Cell. Biol.* **116**, 559-571 (1992).
- Schulze, B., Mann, K., Battistutta, R., Wiedemann, H. & Timpl, R. Structural properties of recombinant domain III-3 of perlecan containing a globular domain inserted into an epidermal-growth-factor-like motif. *Eur. J. Biochem.* **231**, 551-556 (1995).